CHAPTER-5

Classification of Human Foot Movements for Ankle-Foot Prosthesis Control using Machine Learning and Fuzzy Logic Techniques

Highlights of the Chapter

- *EMG and FMG sensors*
- *Raspberry Pi and Arduino Nano 33 BLE controllers*
- *Machine learning algorithms for foot movement classification*
- *TinyML based portable computing system*
- *Fuzzy logic for foot movement*

ABSTRACT

Purpose – This paper presents different machine learning techniques to classify the following foot movements: (i) dorsiflexion, (ii) plantarflexion, (iii) inversion, (iv) eversion, (v) medial rotation, and (vi) lateral rotation. The purpose is to design a real-time standalone computing system to predict the foot movements in the sagittal plane, useful for ankle-foot prosthesis control.

Design/methodology/approach– Myoelectric and force-myography signals have been acquired from the leg's tibialis anterior, medial gastrocnemius, lateral gastrocnemius, and peroneus longus muscles. Raspberry Pi, an embedded type affordable computer, was used to acquire the two signals, followed by their application in the classification of foot movements in real-time. The MCP3008, 10-bit analog-to-digital converter, was interfaced with Pi, used to read analog sensor data from the sensors. Later, an Arduino Nano 33 BLE controller was employed to implement the TinyML algorithm in the

Arduino environment to classify these foot movements. The labeled data was used for the controller's training and afterward trained system was used to classify foot movement from real-time acquired signals. Arduino Nano 33 BLE is also used to implement fuzzy logic rules to accomplish ankle-foot movement classification tasks. Finally, the real-time classification of dorsiflexion, flat-foot, and plantarflexion is applied to generate a signal for controlling the ankle-foot prosthesis for the below-knee amputees.

Findings – The results showed that Raspberry Pi-based classification provided more than 99.5% accuracy for the EMG signals using LDA, LR, KNN, and SVC classifiers for offline prediction. However, for the classification of real-time signals, the performance of LDA is exceptionally well in predicting all classes. Further, the classification accuracy using EMG signal is much better than FMG based classification. Arduino Nano 33 BLE controller is also tested with TinyML based neural network algorithm for foot movement classification. It is observed that even a two-layer neural network performed the classification task in real-time (8.5msec) without any misclassification. Finally, the data is collected from the amputee's residual limb, and after training a model, predicted response is checked, and it is found that all three classes were classified correctly. Our finding suggests that a TinyML based Arduino Nano 33 BLE microcontroller is comparatively faster to predict and control, and it is smaller in size, thus advantageous for real-time prosthetic leg control applications. Also, the real-time results obtained using TinyML technique are better than fuzzy logic classifiers in terms of prediction accuracy.

Practical implications – This study presents the realization of subject intent for different foot movements. Furthermore, two different real-time portable systems have been designed and realized; those are useful for controlling a lower limb prosthesis, mainly to mimic the functioning of ankle-foot.

Originality/value – The EMG signals were collected from below-knee muscles to classify different foot movements using Raspberry Pi and Arduino Nano 33 BLE controllers. The ML algorithms were tested on healthy and amputee subjects using these portable devices. The results showed the applicability of ML techniques to control the ankle-foot prosthetic prototype and other prosthetic control applications.

5.1 Introduction

The lower limb muscle activity has a significant role in body control. Therefore, it is advantageous to monitor the lower limb muscle activity for realizing the body condition, and it may be helpful while designing and controlling the prosthetic ankle-foot. Due to the exchange of ions across muscle fiber membranes, small electrical currents are produced by muscle fibers preceding muscle force production. This signal is called the electromyogram (EMG). It can be measured using surface electrodes on the skin surface (Day, 2002). Surface electromyography (sEMG) is a widely used tool to investigate muscle activity. The sEMG electrodes can be embedded in the prosthesis socket to provide a non-invasive technique to record the residual limb's muscles' electrical activity. The movements associated with the human ankle-foot complex, such as dorsiflexion, plantarflexion, inversion, eversion, medial rotation, and lateral rotation, are the primary activities in our daily life. Consequently, these are extensively utilized in rehabilitation workouts and examine the locomotor tasks of weak individuals (Jiang *et al.*, 2016).

Exoskeletons and orthoses are mechanical wearable devices that are humanlike and perform according to the operator's movements (Herr, H., 2009). The term 'orthosis' typically describes a device used for the assistance of people with limb pathology. Adiputra *et al.* (2019) presented the gait control strategy for ankle-foot orthosis (AFO). An AFO assists the patients with foot drop problems. The AFOs may have a fixed joint (rigid AFO), more flexible joint (flexible rigid AFO), and freely rotating ankle joint

(articulated AFO). Numerous actuating devices such as solenoids, springs, DC motors, pneumatic mechanisms, oil dampers, magnetorheological (MR) dampers, MR brakes are available that controls the gait. A healthy gait can be replicated on such patients by controlling the ankle joint (especially bending stiffness, damping stiffness, assistive torque, and motion path) using such a mechanism. The term 'exoskeleton' describes a device that increases the performance of a non-disabled wearer. Al-Quraishi *et al.* (2017) used EMG signal-based pattern recognition for robotic exoskeleton applications.

Other than EMG, the researchers have utilized joint angle sensors, inertial measurement units (IMUs), force-sensitive resistor (FSR), and other sensors for wearable gait analysis, prosthetics, and other applications. For example, Eilenberg *et al.* (2010) presented an adaptive muscle-reflex controller for ankle-foot prosthesis, where the model's parameters match the human ankle's torque-angle profile. The authors used a hall-effect sensor on the ankle joint to measure the angle, whereas strain gauges were fitted inside the prosthetic pyramid assembly to estimate torque at the ankle joint. Archer *et al.* (2014) presented an outline for sitting, standing, lying, walking, and running activity classification using inertial measurement unit (IMU) sensors mounted on AFOs. Malesevic (2011) proposed an IMU-based system to detect and classify foot movement using the k nearest neighbors classification technique. In another application to detect footsteps, IMU-based pedometers are perfect for moderate and faster walking steps detection; but the accuracy can be unacceptable for low walking speed (the case of older adults). Chu *et al.* (2017) presented the force-myography (FMG) strap-based wearable step detection system that is reported feasible at low speeds.

Many researchers have introduced FMG in upper limb prostheses (Connan *et al.*, 2016; Delva *et al.*, 2010). Authors reported that FMG displays better stability over time than

sEMG to enhance the functionality and controllability of prosthetic hands. There is a variation in the volume of the underlying muscle for any limb movement; therefore, the force generated at the limb surfaces changes. This force is recorded by force-sensitive resistor (FSR) sensors embedded into a band. Jiang *et al.* (2016) employed these FSR sensors on the distal end of the lower limb for detecting ankle position. The signals were recorded corresponding to various ankle movements. The authors obtained 94% cross-validation and 85% cross-trial evaluation using a linear discriminant analysis classifier. In another work, Jiang *et al.* (2018) have used FMG to predict four gait phases for the treadmill walk. Godiyal *et al.* (2019) investigated the FMG patterns for five locomotion modes. The authors used a flexible strap around the thigh with evenly placed FSR 400 sensors at the inner periphery of the strap. Xiao and Menon (2019) presented a recent review on the research and development of FMG technology in the last 20 years.

Recently, hybrid sensor technology such as EMG-electroencephalography (EEG) (Hooda *et al.*, 2020), and EMG-accelerometer (Negi *et al.*, 2020), EMG-FMG (Sharma *et al.*, 2020) have been realized to generate control signals for prosthetic applications. Di Nardo *et al.* (2013) recorded EMG signals from gastrocnemius lateralis and tibialis anterior (TA) muscles for healthy gait to depict the activation modalities of these muscles. Primarily, two activations were found for gastrocnemius lateralis muscles: the first during the flat-foot to push-off transition and the second during mid-swing. Three activations were primarily observed for TA muscles: the first at the beginning of the gait cycle, the second at stance to swing transition, and the third during a terminal swing. In the present study, four below-knee muscles are selected due to the future target of controlling the ankle-foot prostheses. The EMG and FSR sensor data are collected from TA, medial gastrocnemius (MGAS), lateral gastrocnemius (LGAS), and peroneus longus (PL) muscles. The authors aim to design a standalone embedded device-based system that can acquire EMG/FMG

data from the above muscle locations and predict the foot movement accurately using Machine Learning (ML) trained model in nearly real-time.

5.2 Materials and Methods

5.2.1 Human Lower-Limb Motion

Anatomical reference planes consist of 3-imaginary cardinal planes that divide the mass of a body into 3-dimensions. First, the sagittal plane splits the body vertically into left and right halves of equal mass. Second, the frontal plane divides the body vertically into front and back halves. Finally, the horizontal plane separates the body into top and bottom halves (Hall and Lysell, 1995). Ankle joint consists of the tibia, fibula, and underlying tarsal bones. The ankle permits the foot for the following movements: dorsiflexion, plantarflexion, inversion, eversion, medial rotation, and lateral rotation. These basic movements are shown in Figure 5.1. Sagittal plane rotation at the ankle occurs when the foot is moved relative to the lower leg and vice-versa. When a person moves the top of the foot toward the shin, it is called dorsiflexion. While raising the heel off the ground as go up on the ball of the foot, the movement is termed as plantarflexion. Eversion and inversion are the frontal plane movements of the foot. The outward rotation of the sole is termed eversion, and the inward rotation of the sole is called inversion. When the leg is rotated toward the midline of the body in the transverse plane, it is called medial rotation, and when the rotation is away from the body's midline, it is termed lateral rotation.

Agonist and antagonist kinds of muscles exist in human joints such as the hip, knee, and ankle. In addition, several muscles usually activate such a human joint. The skeletal muscles can be divided into mono-articular and bi-articular. A movement can be generated in only one joint for mono-articular muscles, whereas movement can be created in two adjacent joints for bi-articular muscles (Zagrodny *et al.*, 2018). For example,

dorsiflexion/plantarflexion motion of the human ankle joint is mainly actuated by the gastrocnemius, soleus, and tibialis anterior muscles. Here, the only gastrocnemius is the bi-articular muscle, and it works on both the ankle and knee joints. The below-knee muscle activities have been investigated during daily ankle-foot movements such as dorsiflexion, plantarflexion, inversion, eversion, medial rotation, and lateral rotation to control the power-ankle-foot prosthesis based on the muscle's electromyographic (EMG) signals.

Figure 5.1 *Foot movements: dorsiflexion and plantarflexion, eversion and inversion, lateral and medial rotation*

Monitoring the ankle-foot movements is beneficial in many applications such as gait analysis, rehabilitation, and sports injury prevention. In addition, the activation pattern of lower-limb muscles can estimate the human intention for lower-limb movement. He *et al.* (2007) studied the EMG patterns for the daily motion activities such as squatting, sitting down, walking, ascending stairs, and descending stairs. The authors suggested these

findings helpful in designing the lower-limb power-assist robotic systems controllers for physically weak people. Isezaki *et al.* (2019) developed a sock-type system for assessing lower leg muscle activity by placing EMG electrodes at the distal end around the ankles. In our past work (Negi *et al.*, 2021), the FSR and IMU sensors were used for gait phase detection, and the results were correlated with EMG sensors for different terrain locomotion. EMG represents the neural information, hence offers an intuitive way of control. Further, EMG occurs before the actual mechanical movement of the human body; therefore, there is a lag in the output of mechanical sensors, like IMU sensors. In this way, the classifier utilizing the EMG signal will have extra time for the classification of locomotion modes; as a result, a quick response can be achieved.

5.2.2 Data Acquisition

In the present work, two kinds of sensors were studied for the classification of different foot movements. In the First experiment for EMG signal acquisition, four MyoWare muscle sensors (MyoWare Muscle Sensor, 2021) were placed on the four below-knee muscles- TA, MGAS, LGAS, and PL to make four-channel EMG signals. The location of EMG sensors is defined as per the project- sEMG for the non-invasive assessment of muscle (SENIAM) (Hermens *et al.*, 2000). Gel-based (wet) sEMG electrodes were used with MyoWare sensors to attach to these locations. Figures 5.2 and 5.3 show the average (± standard deviation) plot of 100 trials of a subject acquired from above muscles positions for EMG and FMG signals, respectively. In the Second experiment for FMG signal acquisition, four FSR sensors (Interlink Electronics, 2021) were placed on the same site to record FMG signals. Four FSR 402 sensors were fitted on an elastic belt tied to the shank with hook and loop fasteners.

Hardware specifications used to record and analyze the sensor data are Raspberry Pi 3 (model B+ with 1GB RAM) and Arduino Nano 33 BLE microcontroller. Five healthy

subjects (4 male and 1 female) and one transtibial amputee participated in the present study. Initially, the foot is in Foot-flat (FF) position. Other classes are the following six movements from rest position: dorsiflexion (DF), plantarflexion (PF), inversion (IN), eversion (EV), medial rotation (MR), and lateral rotation (LR). A total of 100 trials were collected for each subject for the above 7-classes. The 80% samples of each class were used to train a different ML model, whereas 20% were used to test the model. The ML model that provided more than 95% testing accuracy was later used for real-time prediction in Raspberry Pi and Arduino Nano 33 BLE controllers.

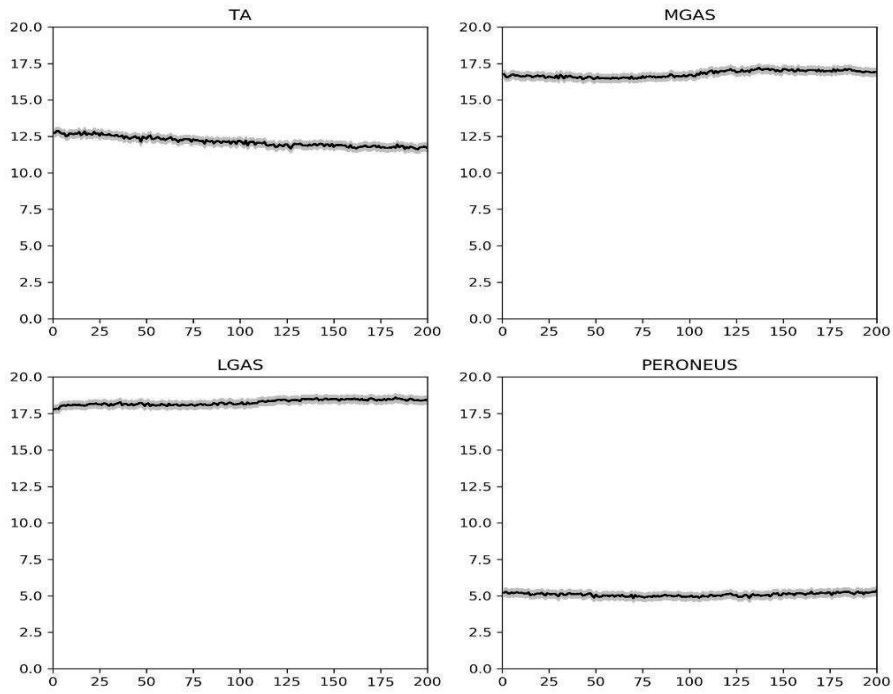

(a) FF

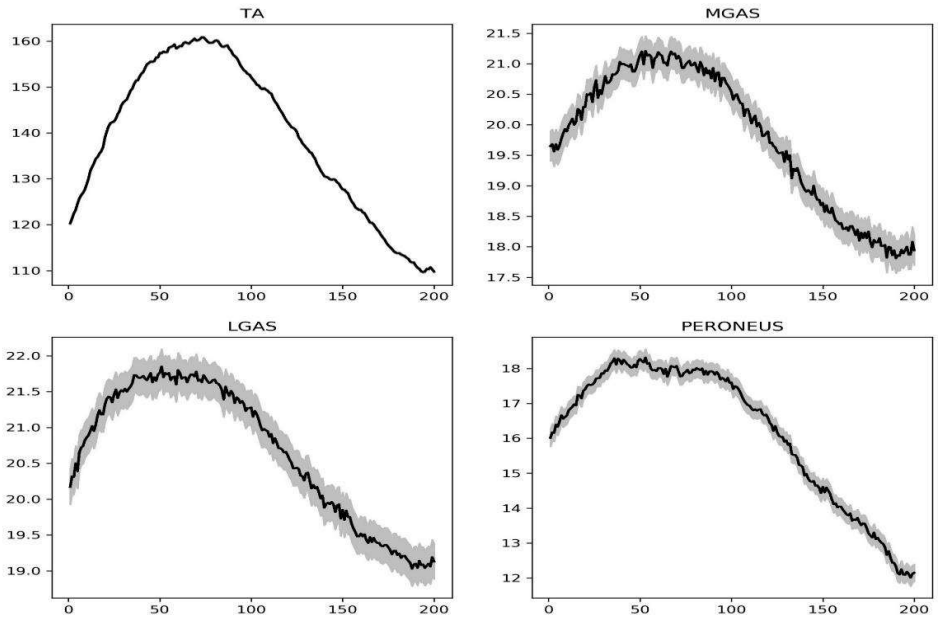

(b) DF

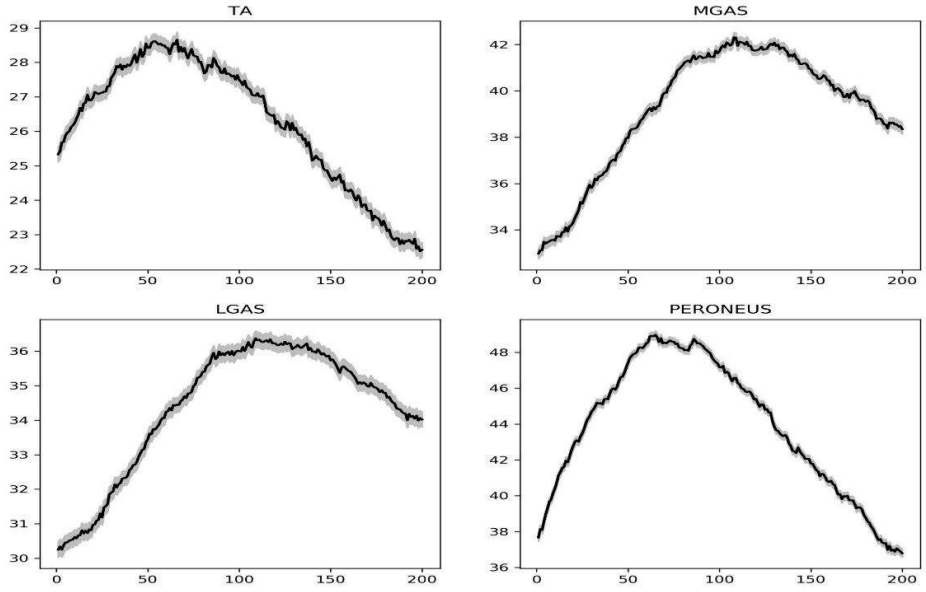

(c) PF

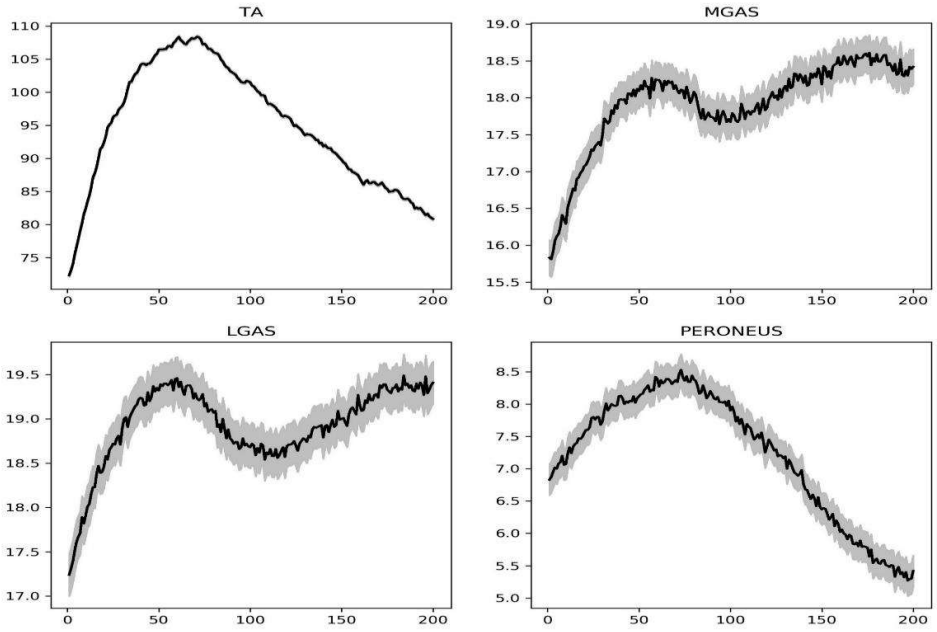

(d) IN

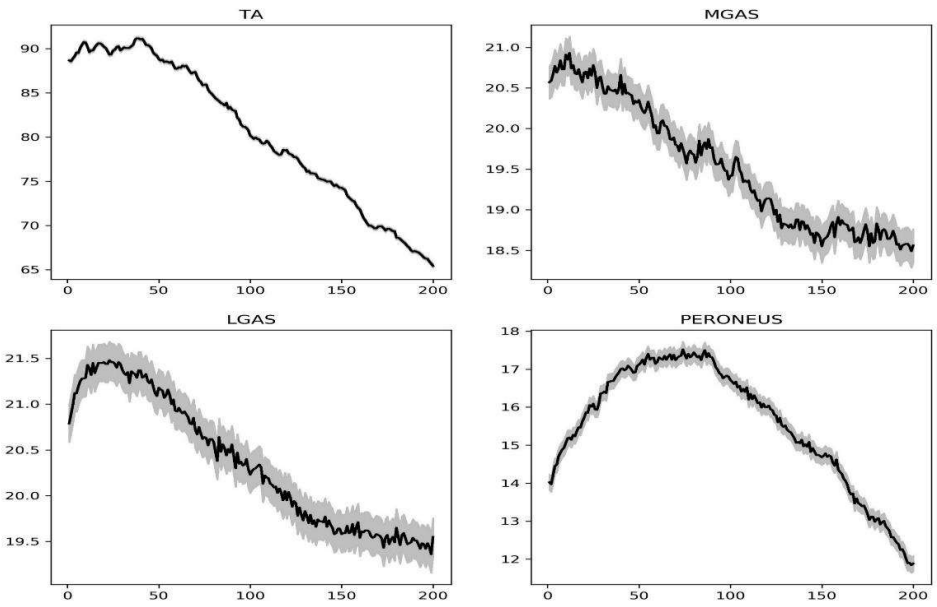

(e) EV

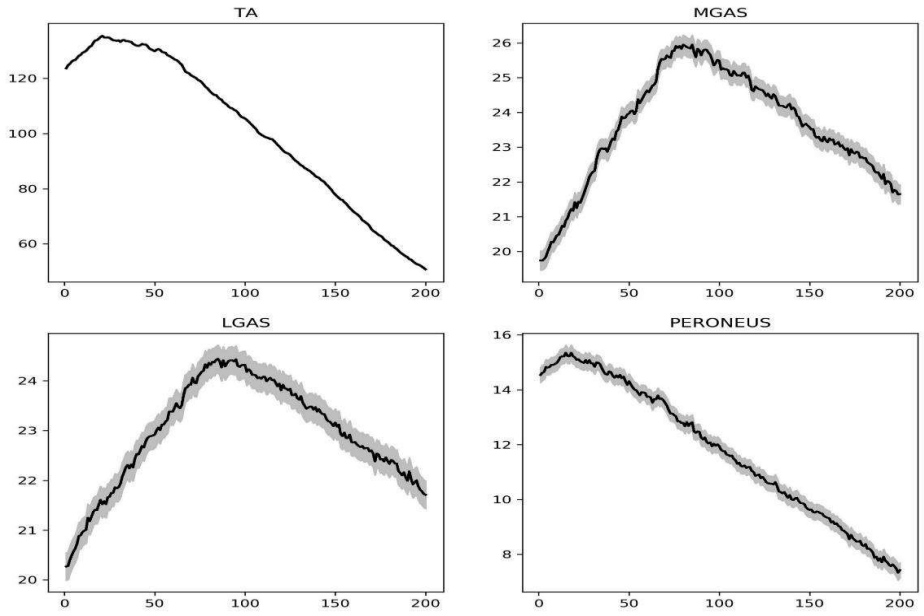

(f) MR

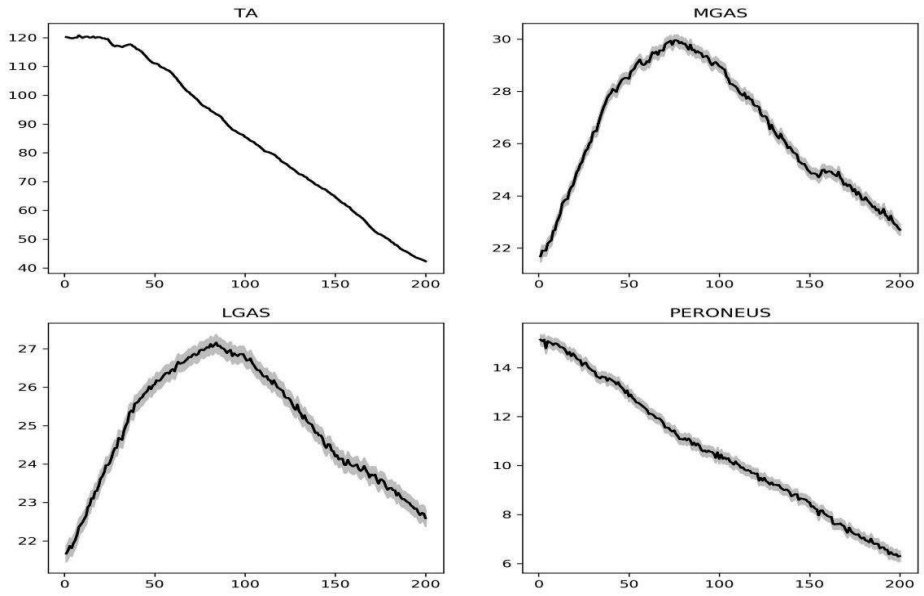

(g) LR

Figure 5.2 Average *EMG patterns for a subject for different foot positions: (a) FF, (b) DF, (c) PF, (d) IN, (e) EV, (f) MR, and (g) LR*

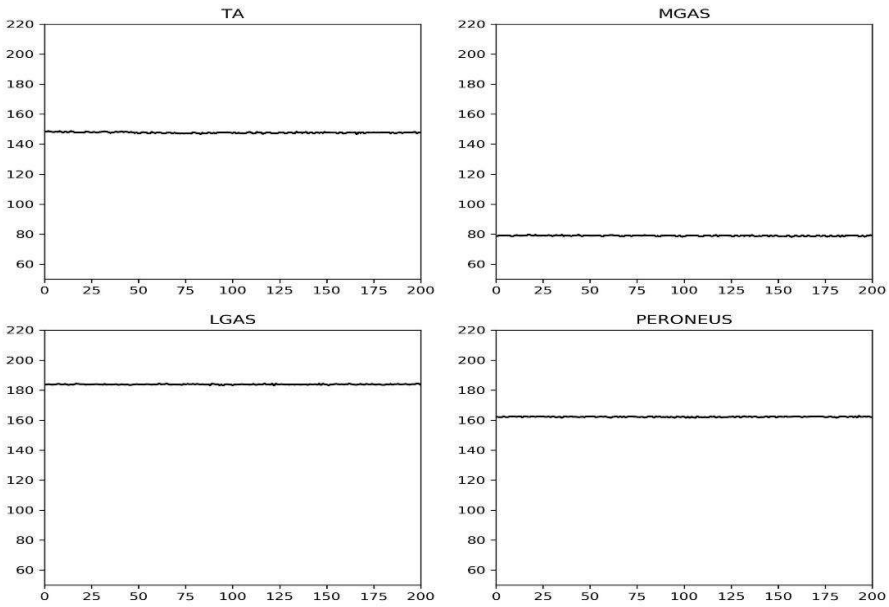
TA
MGAS
LGAS
PERONEUS
220
200
180
160
140
120
100
80
60
0
25
50
75
100
125
150
175
200

(a) FF

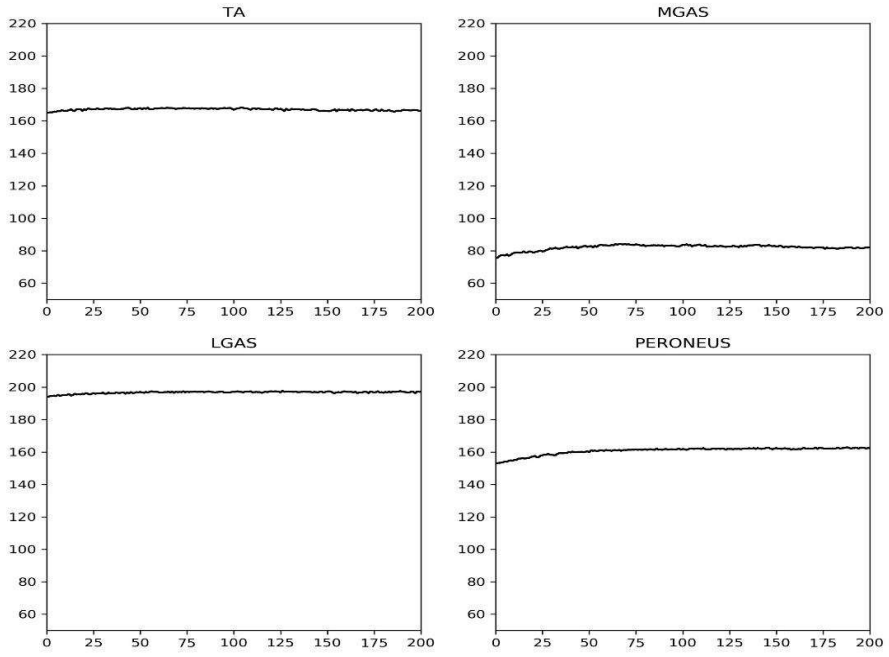
TA
MGAS
LGAS
PERONEUS
220
200
180
160
140
120
100
80
60
0
25
50
75
100
125
150
175
200

(b) DF

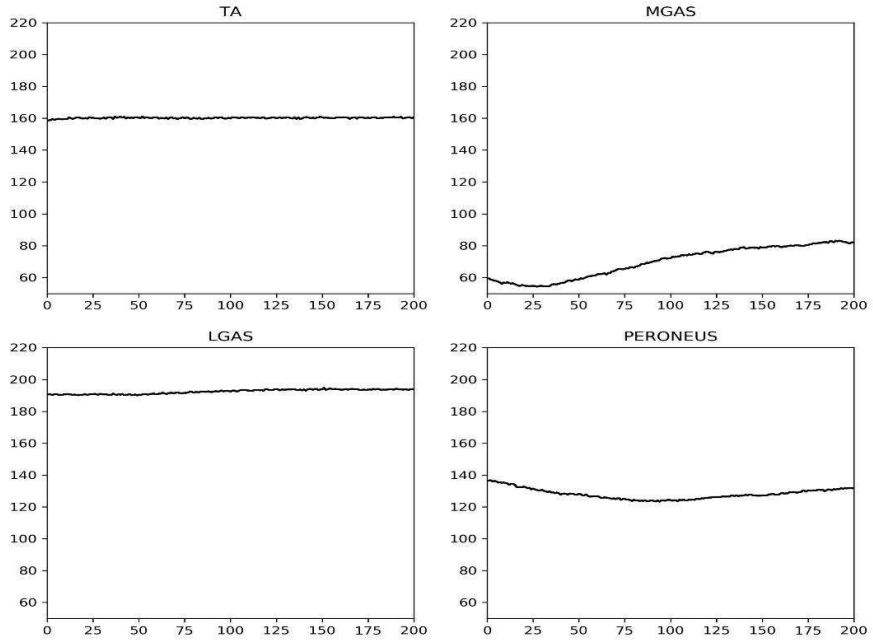
TA
MGAS
LGAS
PERONEUS
220
200
180
160
140
120
100
80
60
0
25
50
75
100
125
150
175
200

(c) PF

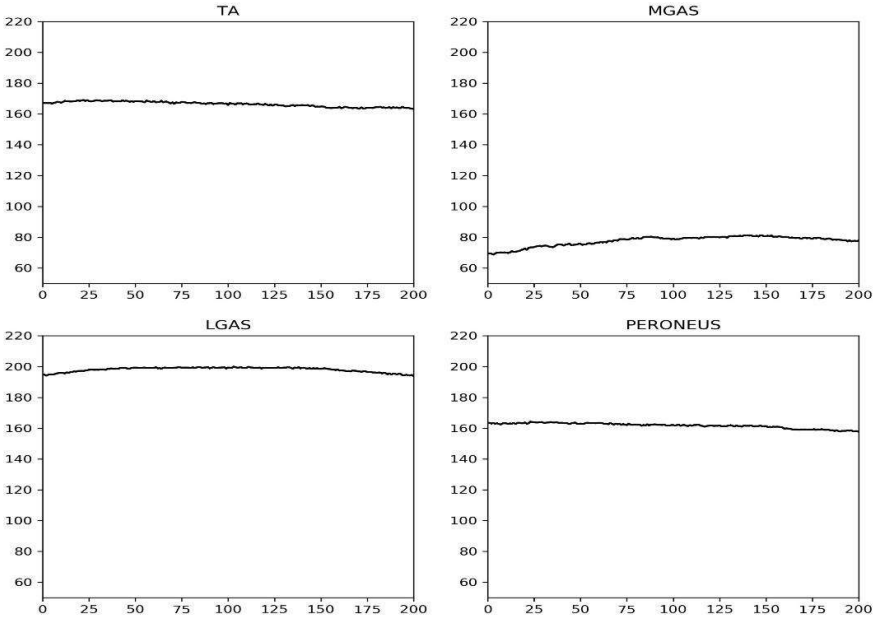
TA
MGAS
LGAS
PERONEUS
220
200
180
160
140
120
100
80
60
0
25
50
75
100
125
150
175
200

(d) IN

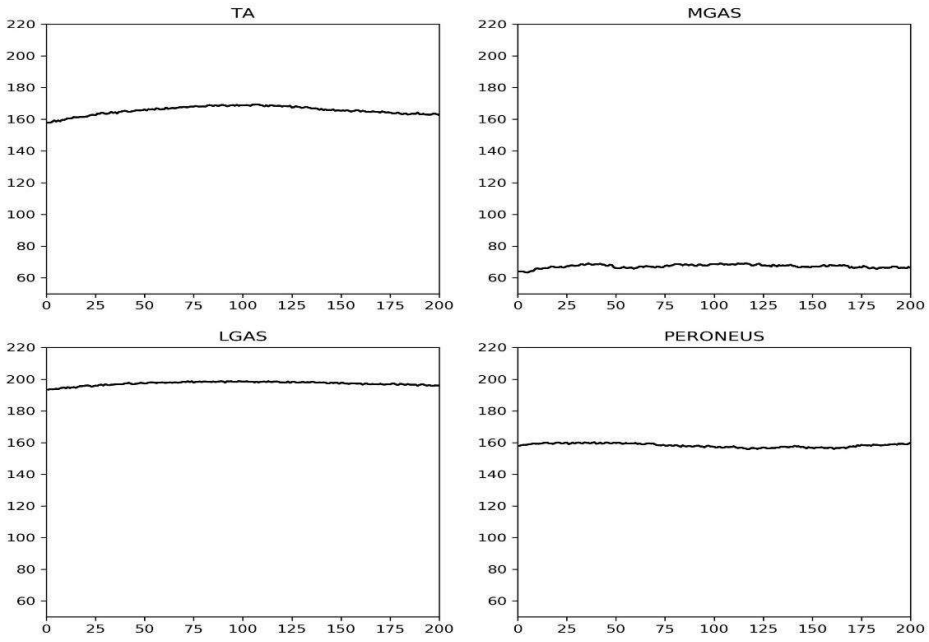
TA
MGAS
LGAS
PERONEUS
220
200
180
160
140
120
100
80
60
0
25
50
75
100
125
150
175
200

(e) EV

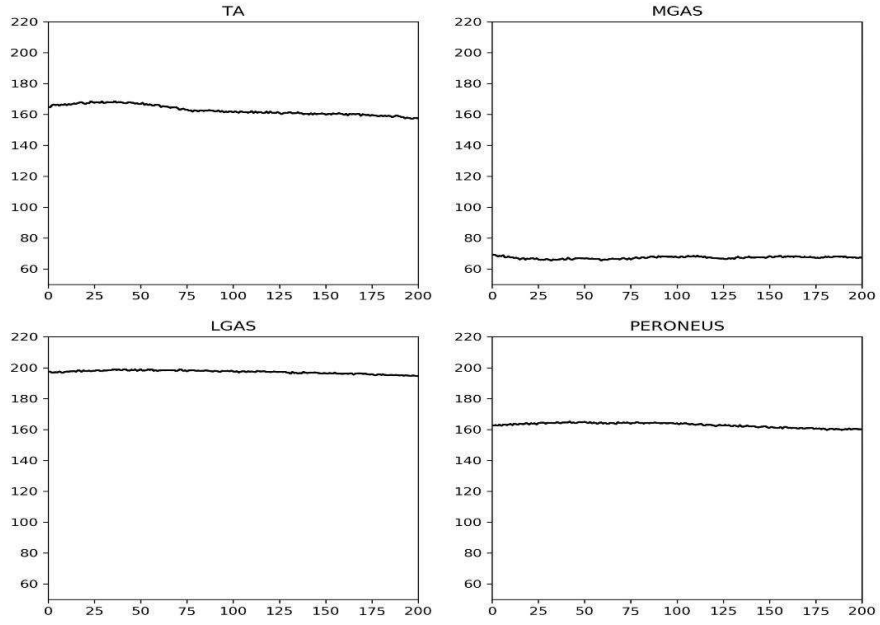
TA
MGAS
LGAS
PERONEUS
220
200
180
160
140
120
100
80
60
0
25
50
75
100
125
150
175
200

(f) MR

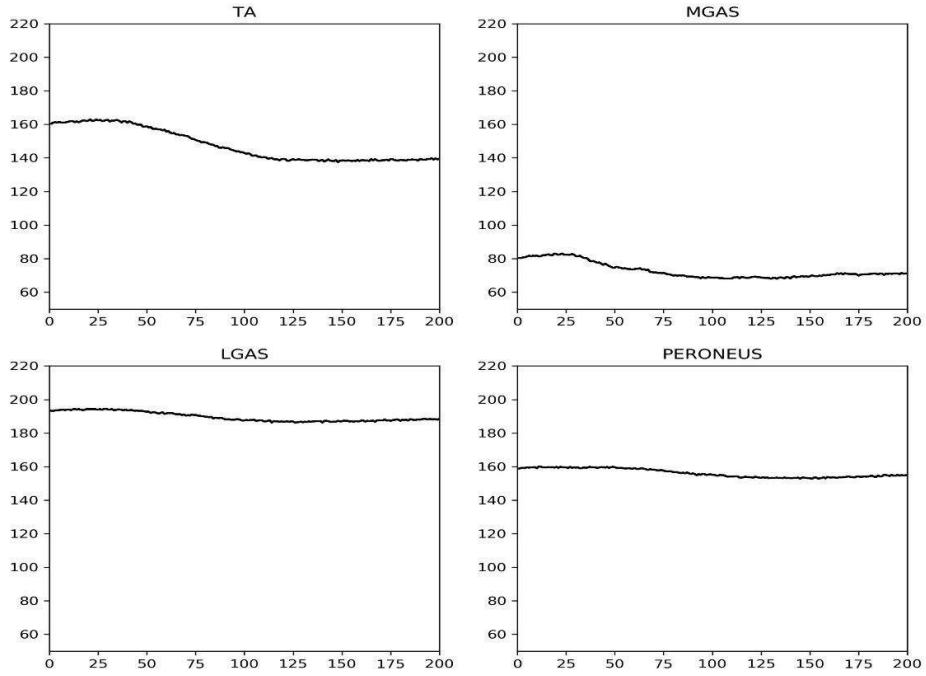

(g) LR

Figure 5.3 Average *FMG patterns for a subject for different foot positions: (a) FF, (b) DF, (c) PF, (d) IN, (e) EV, (f) MR, and (g) LR*

5.2.3 Machine Learning Approaches for Movement Classification

Figure 5.4 shows a generalized workflow diagram for ML techniques to predict foot movement in real-time. The application of Raspberry Pi and Arduino Nano 33 BLE controllers results in high functionality and low cost. In addition, it makes available the facility to employ artificial intelligence (AI) and advanced signal processing methods. It most prominently houses pattern recognition-based control schemes that improve robustness (Oskoei and Hu, 2007). In pattern recognition-based control systems, the desired classes are distinguished using signal patterns with the help of classifiers, and the variety of functions depends directly on the performance of classification. As shown in Figure 5.4, the EMG or FMG database is split into training and testing datasets. A time-

domain feature set (Negi *et al.*, 2016; Negi *et al.*, 2020) containing root mean square, integrated absolute value, modified mean absolute value, and waveform length features is used. After getting proper validation accuracy, the model is ready to predict the real-time foot movement of the subject.

A total of 10 different classifiers are used to examine the classification performance for the prediction of desired foot movement. These classifiers are Linear Discriminant Analysis (LDA), Logistic Regression (LR), K Nearest Neighbors (KNN), Support Vector Classification (SVC), Gaussian Naive Bayes (GNB), Decision Tree (DT), Random Forest (RF), Multi-Layer Perceptron (MLP), Gradient Boosting (GB), and AdaBoost (AB). Scikit-learn, an integrated Python module, is used to build these ML algorithms (Pedregosa *et al.*, 2011). Once the model is trained using an ML algorithm, it is saved with pickle operation, also called serialization; later, this pickle file is deserialized to make new predictions on new data. These saved models can be imported into Raspberry Pi, and for new data, it predicts the current class in real-time. Similarly, the neural network algorithm is implemented and tested on Arduino Nano 33 BLE environment to make TinyML based standalone system useful for real-time ankle-foot prosthesis control.

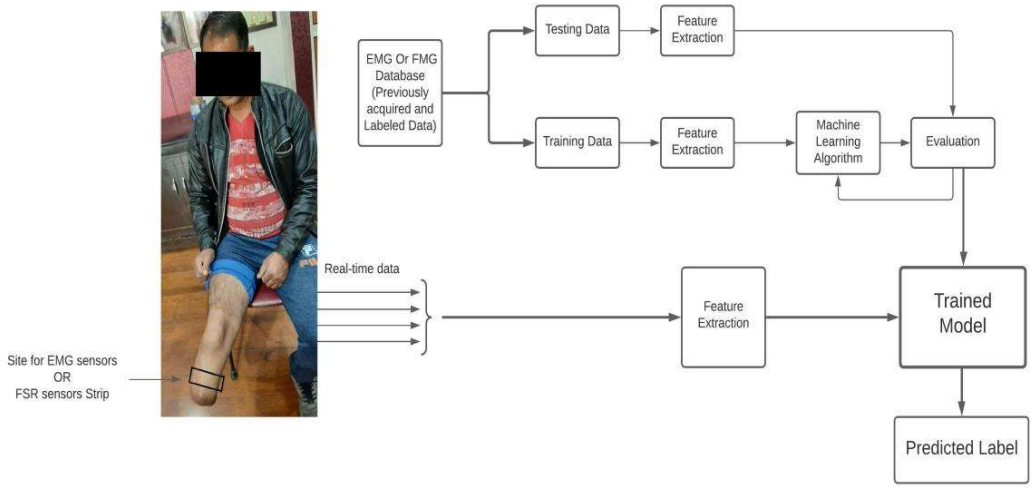

Figure 5.4 *ML-based foot movement prediction for ankle-foot prosthesis control*

5.2.4 Ankle-Foot Prosthesis Control in Sagittal Plane

The ML classifiers algorithms implemented on Raspberry Pi and Arduino Nano 33 BLE controllers have been used to classify three-foot positions: dorsiflexion, foot-flat, and plantarflexion. A real-time prediction is used as a control signal to actuate the motor that controls the movement of the ankle-foot prosthesis in the sagittal plane. Figure 5.5 shows the block diagram of the Arduino Nano 33 BLE controller-based interface with encoder DC servo motor utilizing I2C protocol for both EMG and FMG sensors as the input signal. The four muscle sites used in this study find their suitability for predicting above three-foot positions for both signals. The predicted class output as FF, DF, and PF provides the control signal to bring the motor at an absolute zero position, rotate the motor clockwise, and rotate the motor counterclockwise. High torque encoder DC servo motor and driver (RHINO MOTION CONTROLS, 2021) provides the dorsiflexion and plantarflexion movements of the prosthetic foot.

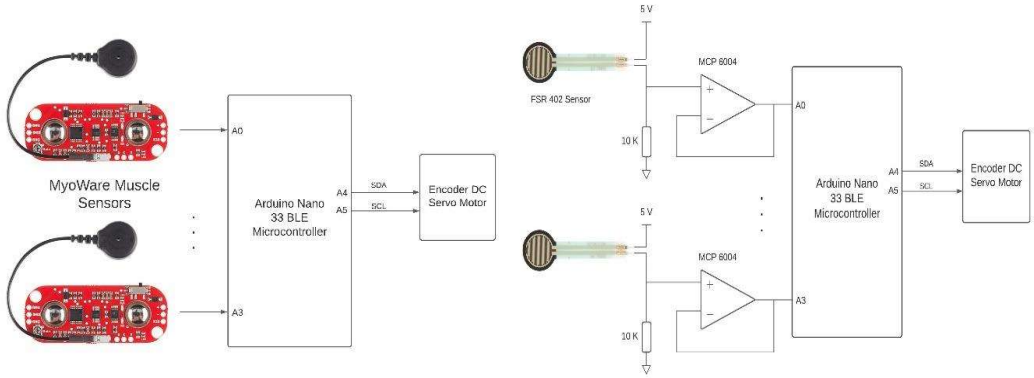

(a) *(b)*

Figure 5.5 *Encoder DC servo motor control using: (a) EMG sensors, (b) FSR sensors*

The ankle-foot prosthesis, as shown in Figure 5.6, consists of two major control parts: at the rear end of the prosthetic foot, there exists an MR damper whose damping is controlled by varying the current; another part is the motor actuator which is used to

provide the movement in the sagittal plane. When the foot is in the air during the swing phase, the motor is turned on to rotate the foot so that the toe faces up, and it helps to provide a good heel strike during the initial contact of the stance phase. As the heel strikes the ground, the MR damper is active, and maximum current flows through the damper. For foot flat motor might be used to bring the foot from dorsiflexion to foot-flat, whereas the damping is reduced. The damper is inactive during toe-off, and the motor is active in the reverse direction to support during toe-off (powered plantarflexion).

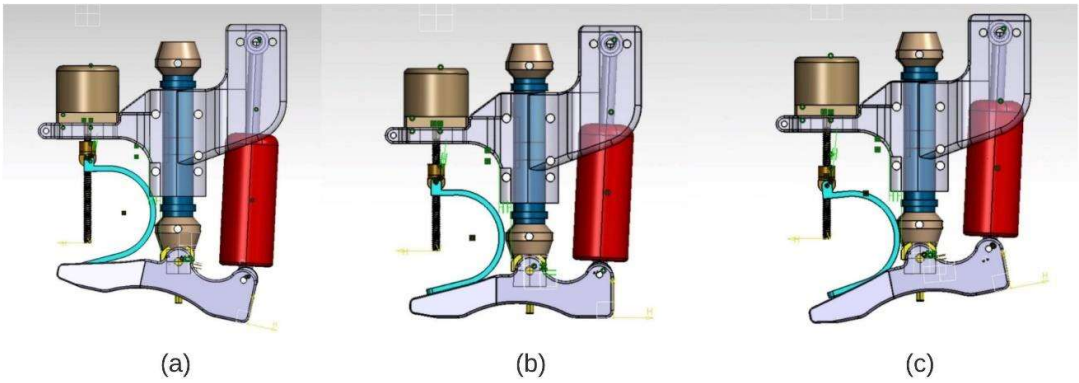

Figure 5.6 *Ankle-foot prosthesis control in sagittal plane: (a) dorsiflexion, (b) foot-flat, and (c) plantarflexion*

5.3 Results and Discussion

5.3.1 Raspberry Pi Based Classification

ML pattern classification is obtained for different classifiers, for the myoelectric signal acquired from four- below-knee muscles. The study incorporates the use of 10 classifiers for three, five, and seven-foot movement classifications. Out of these, the three-class pattern recognition is used to control ankle-foot prostheses in the sagittal plane, thereby supporting the dorsiflexion, foot-flat, and plantarflexion movements. Table 5.1 shows the classification results for the three-class pattern recognition using 10 different classifiers for EMG data, where it is observed that most of the classifiers are suitable to classify

three-pattern recognition tasks having accuracy between 99 and 100%. The LDA, LR, KNN, and SVC classifiers outperformed other classifiers; however, when the model is tested in real-time on subjects, it is observed that for most of the classifiers, some classes were misclassified; however, only the LDA classifier provided the best prediction for all classes. The Raspberry Pi took approximately 10 sec to start, and after that, it provides each real-time prediction in 20msec.

Table 5.1 *ML Classifier performance for three sagittal plane foot positions [for EMG]*

Classifier	Accuracy (%)	Precision	Recall	f1-score
LDA	99.583 (±0.722)	0.996 (± 0.008)	0.996 (± 0.008)	0.996 (±0.008)
LR	100.000 (±0.000)	1.000 (± 0.000)	1.000 (± 0.000)	1.000 (±0.000)
KNN	100.000 (±0.000)	1.000 (± 0.000)	1.000 (± 0.000)	1.000 (±0.000)
SVC	100.000 (±0.000)	1.000 (± 0.000)	1.000 (± 0.000)	1.000 (±0.000)
GNB	98.473 (±2.644)	0.987 (± 0.023)	0.984 (± 0.027)	0.986 (±0.025)
DT	97.777 (±3.851)	0.981 (± 0.033)	0.979 (± 0.037)	0.979 (±0.037)
RF	99.443 (±0.964)	0.996 (± 0.008)	0.996 (± 0.008)	0.994 (±0.010)
MLP	99.167 (±1.100)	0.992 (± 0.011)	0.992 (± 0.011)	0.991 (±0.010)
GB	99.443 (±0.964)	0.994 (± 0.010)	0.994 (± 0.010)	0.994 (±0.010)
AB	98.473 (±2.644)	0.987 (± 0.023)	0.984 (± 0.027)	0.986 (±0.025)

However, from Figure 5.7, it can be seen that as the classes increase, the classification accuracy and other performance metrics decrease. Few classifiers, such as SVC, KNN, RF, and MLP, are suitable for classifying the 5-class and 7-class classification tasks. However, if we acquire the input signal using more channels at suitable muscle sites, the performance metrics can be improved. Table 5.2 shows the confusion matrix and other performance evaluation metrics of the SVC classifier for a randomly chosen subject-2 to classify three different class pattern recognition problems.

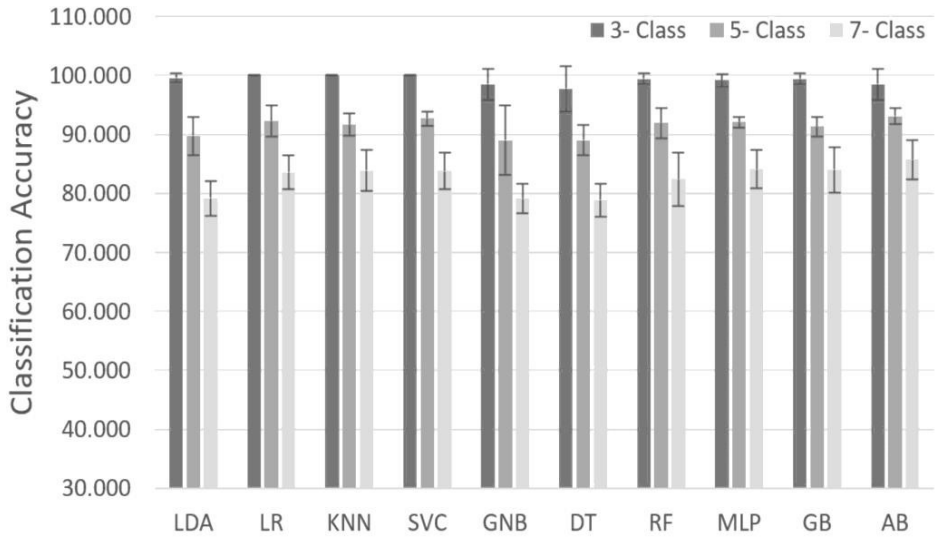

Figure 5.7 *Classification accuracy for 3, 5, and 7-foot positions using different classifiers for EMG*

Table 5.3 shows the classification accuracy comparison for different ML classifiers, where the input signal is based on FMG. For 3-class classification, the results showed that FMG could be used as an alternative method for EMG signals. Here again, the LDA classifier provided the real-time applicability for Raspberry Pi for ankle-foot position control. However, if the results of these EMG and FMG-based datasets were compared, it is seen that for 5-class and 7-class pattern classification tasks (Figure 5.7 and 5.8), the EMG signal is more powerful.

Table 5.2 *Confusion matrix and performance evaluation metrics for SVC classifier to classify foot positions using subject-2 EMG signals: (a) 3-class, (b) 5-class, and (c) 7-class*

	FF	DF	PF
FF	80	0	0
DF	0	80	0
PF	0	0	80

	precision	recall	f1-score	support
FF	1.0	1.0	1.0	80.0
DF	1.0	1.0	1.0	80.0
PF	1.0	1.0	1.0	80.0

(a) Accuracy: 100%

	FF	DF	PF	IN	EV
FF	80	0	0	0	0
DF	0	77	0	3	0
PF	0	0	80	0	0
IN	0	17	0	61	2
EV	3	0	1	0	76

	precision	recall	f1-score	support
FF	0.96	1.00	0.98	80.0
DF	0.82	0.96	0.89	80.0
PF	0.99	1.00	0.99	80.0
IN	0.95	0.76	0.85	80.0
EV	0.97	0.95	0.96	80.0

(b) Accuracy: 93.50%

	FF	DF	PF	IN	EV	MR	LR
FF	80	0	0	0	0	0	0
DF	0	72	0	8	0	0	0
PF	0	0	79	0	1	0	0
IN	0	15	1	50	2	11	1
EV	3	0	0	0	74	0	3
MR	0	0	0	12	0	60	8
LR	5	0	1	2	3	5	64

	precision	recall	f1-score	support
FF	0.91	1.00	0.95	80.0
DF	0.83	0.90	0.86	80.0
PF	0.98	0.99	0.98	80.0
IN	0.69	0.62	0.66	80.0
EV	0.92	0.92	0.92	80.0
MR	0.79	0.75	0.77	80.0
LR	0.84	0.80	0.82	80.0

(c) Accuracy: 85.53%

Table 5.3 *ML Classifier performance for three sagittal plane foot positions [for FMG]*

Classifier	Accuracy (%)	Precision	Recall	f1-score
LDA	96.387 (±3.129)	0.967 (±0.029)	0.964 (±0.031)	0.963 (±0.032)
LR	95.693 (±5.142)	0.964 (±0.039)	0.957 (±0.051)	0.956 (±0.053)
KNN	96.803 (±5.177)	0.974 (±0.041)	0.968 (±0.053)	0.967 (±0.052)
SVC	94.723 (±6.473)	0.960 (±0.046)	0.947 (±0.066)	0.946 (±0.068)
GNB	94.583 (±6.223)	0.956 (±0.049)	0.947 (±0.062)	0.944 (±0.062)
DT	88.610 (±10.413)	0.923 (±0.067)	0.887 (±0.104)	0.882 (±0.112)
RF	91.667 (±9.769)	0.942 (±0.057)	0.917 (±0.098)	0.909 (±0.109)
MLP	95.693 (±3.938)	0.958 (±0.039)	0.957 (±0.038)	0.956 (±0.040)
GB	89.860 (±10.003)	0.931 (±0.064)	0.899 (±0.100)	0.890 (±0.110)
AB	91.803 (±11.759)	0.948 (±0.069)	0.919 (±0.115)	0.911 (±0.129)

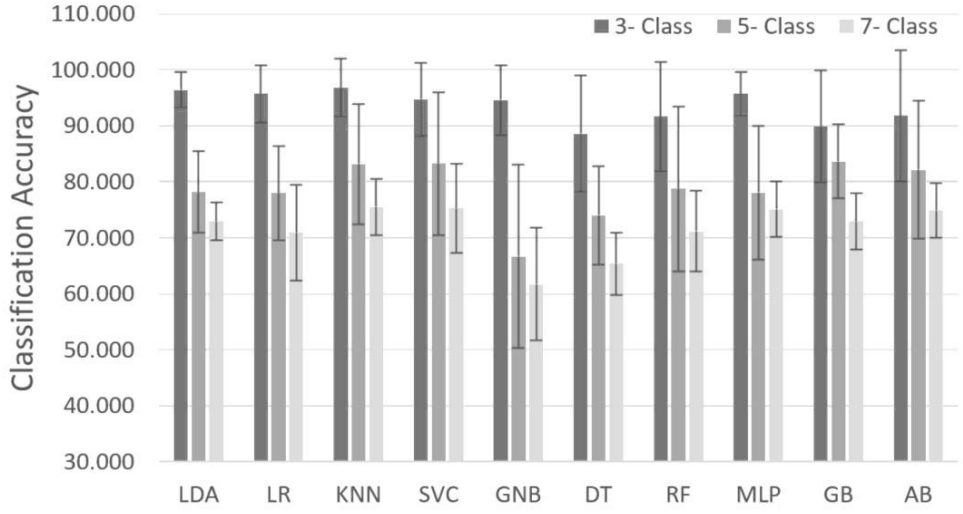

Figure 5.8 *Classification accuracy for 3, 5, and 7-foot positions using different classifiers for FMG*

5.3.2 Arduino Nano 33 BLE based Classification

5.3.2.1 TinyML based prediction

The Arduino Nano 33 BLE is Arduino's 3.3V compatible board with an inbuilt 9-axis IMU sensor. Microcontrollers are small and low-powered computing devices. Bringing ML to such tiny microcontrollers might be feasible to get a real-time standalone system to classify foot movements. TensorFlow Lite is used for running neural network models on such microcontrollers with only a few kilobytes of memory. Different model architectures were used while training the model. As shown in Figures 5.9 and 5.10 for seven different model architectures, there is not much difference in the classification accuracy. So, it is decided to use a two-layer neural network to reduce the computation time and memory. The EMG signal provides better classification as compared to the FMG technique. Here again, as the number of classes is increased for the classification task, the accuracy reduces. It is observed that the Arduino Nano 33 BLE does not take a long time to start as in the case of Raspberry Pi, and it provides each real-time prediction in 8.5 msec.

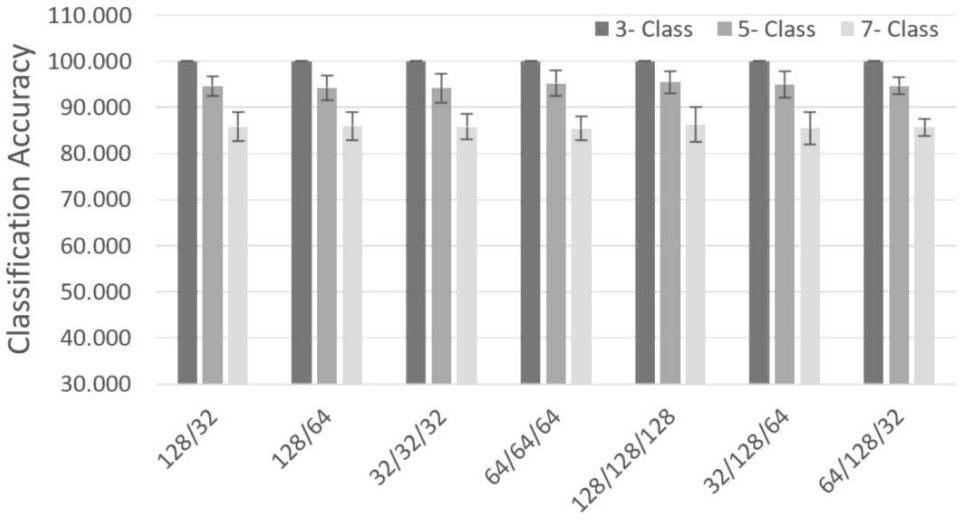

Figure 5.9 *TinyML model performance for the classification of 3, 5, and 7-foot positions using EMG*

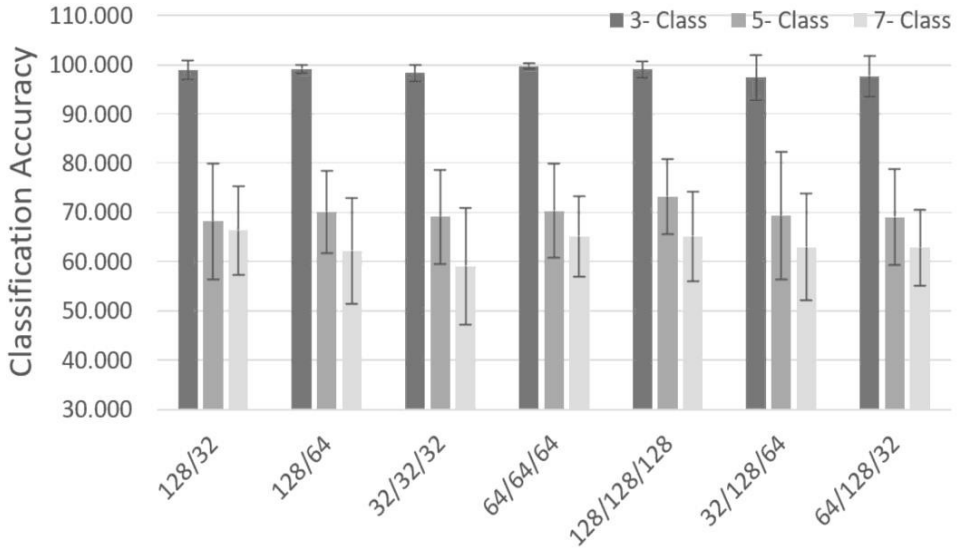

Figure 5.10 *TinyML model performance for the classification of 3, 5, and 7-foot positions using FMG*

Once it is found that Arduino Nano 33 BLE is more advantageous in terms of computation time, faster data acquisition (as the analog channels are inbuilt), and smaller size compared with Raspberry Pi 3 B+, the Arduino Nano 33 BLE is selected to acquire the EMG sensor data from a transtibial amputee using same muscles as used previously. The training and testing results are mentions in Table 5.4 for the amputee.

Table 5.4 *Confusion matrix and performance evaluation metrics for TinyML classifier to classify the foot movements in the sagittal plane for a transtibial amputee*

Accuracy: 97.92%

	FF	**DF**	**PF**
FF	80	0	0
DF	0	79	1
PF	2	2	76

	precision	**recall**	**f1-score**	**support**
FF	0.98	1.00	0.99	80.0
DF	0.98	0.99	0.98	80.0
PF	0.99	0.95	0.97	80.0

5.3.2.2 Fuzzy logic-based prediction

In another experiment, fuzzy logic is also used for the classification of three- foot positions in sagittal plane. Fuzzy results are mentioned for a subject using 50 trials of each class. 80% data is used for training purpose, and remaining 20% is used for testing. Figure 5.11 shows the training data error for foot position classification using EMG signal. Figure 5.12 shows the average testing error for 20% testing data. Table 5.5 presents the prediction accuracy for ten testing trials and their average and standard deviations. Figure 5.13 shows the training data error for foot position classification using FMG signal. Figure 5.14 shows the average testing error for 20% testing data. Table 5.6 presents the prediction accuracy for ten testing trials and their average and standard deviations. Comparing Table 5.5 and 5.6, it can be observed that fuzzy logic provides better accuracy for EMG signal to classify foot movements.

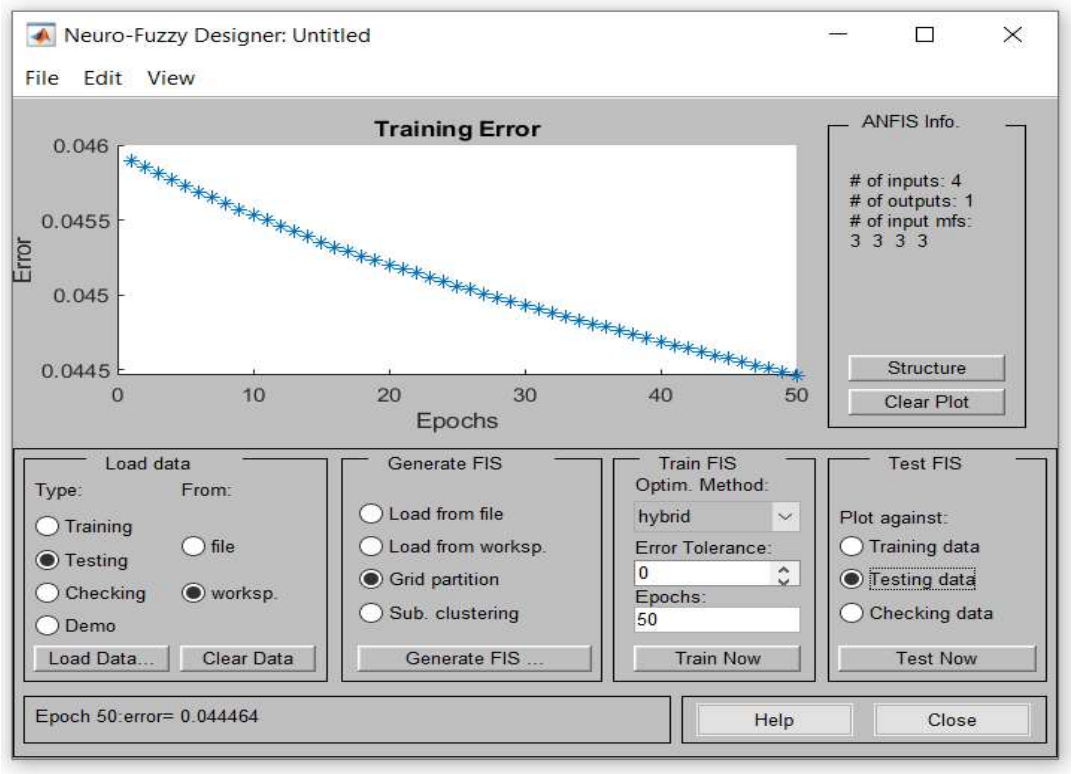

Figure 5.11 *Training data error (Foot movement classification for EMG signal)*

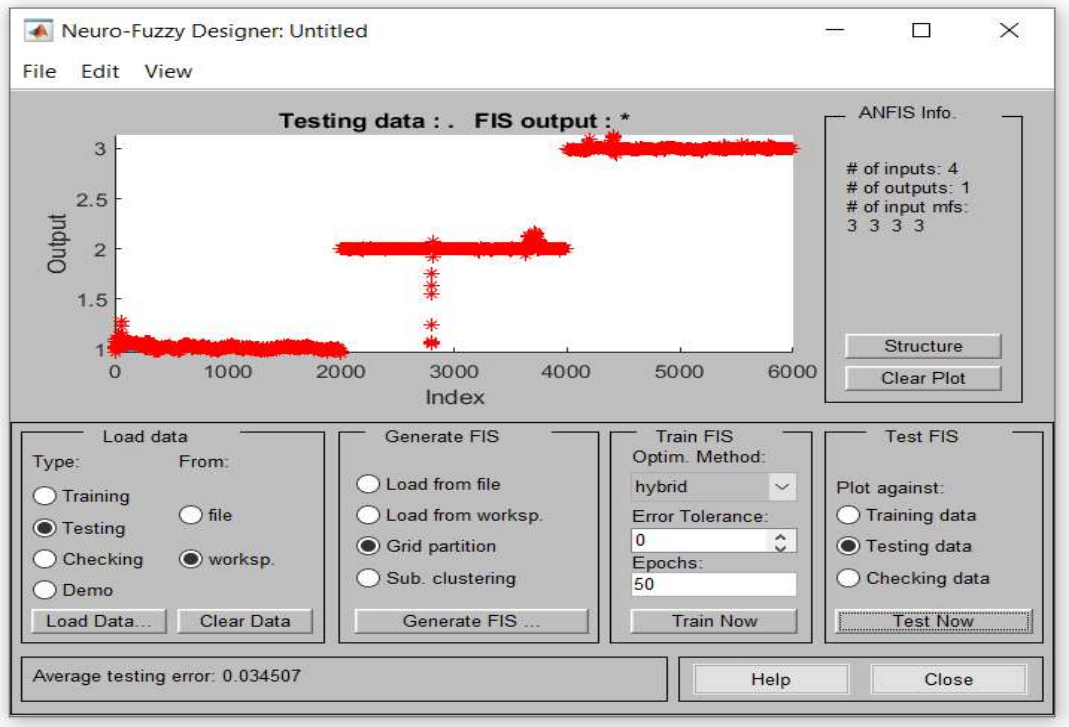

Figure 5.12 *Average Testing data error (Foot movement classification for EMG signal)*

Table 5.5 *Fuzzy logic performance for EMG signal to classify three- foot movements*

Trial #	Absolute Error	Absolute Relative Error	Accuracy (%)
1	0.03	2.24	97.76
2	0.01	1.14	98.86
3	0.01	0.64	99.36
4	0.01	1.11	98.89
5	0.02	0.97	99.03
6	0.01	0.70	99.30
7	0.01	0.36	99.64
8	0.01	0.72	99.28
9	0.02	1.11	98.89
10	0.00	0.35	99.65
Average	**0.01**	**0.93**	**99.07**
Stdev	**0.01**	**0.52**	**0.52**

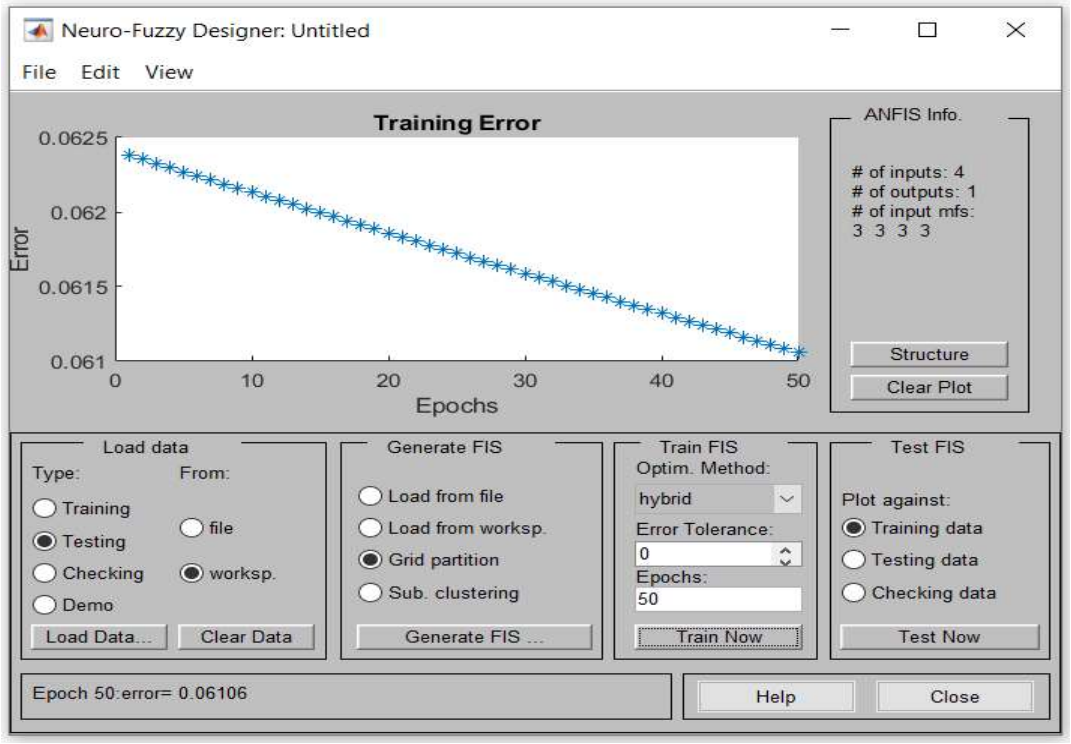

Figure 5.13 *Training data error (Foot movement classification for FMG signal)*

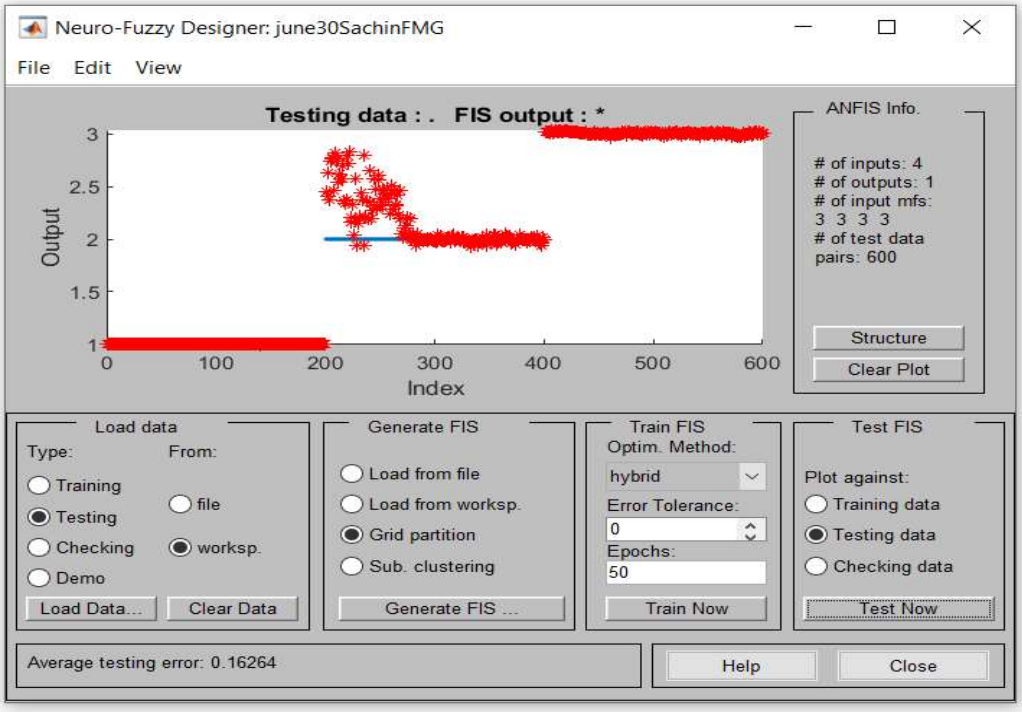

Figure 5.14 *Average Testing data error (Foot movement classification for FMG signal)*

Table 5.6 *Fuzzy logic performance for FMG signal to classify three- foot movements*

Trial #	Absolute Error	Absolute Relative Error	Accuracy (%)
1	0.47	18.72	81.28
2	0.23	11.10	88.90
3	0.16	7.83	92.17
4	0.15	7.24	92.76
5	0.12	5.79	94.21
6	0.10	4.68	95.32
7	0.09	4.41	95.59
8	0.07	3.26	96.74
9	0.11	5.47	94.53
10	0.06	2.87	97.13
Average	**0.16**	**7.14**	**92.86**
Stdev	**0.12**	**4.49**	**4.49**

Indeed, the raw EMG signal needs some post-processing steps such as filtering to control prosthesis that may cause a delay. On the contrary, the force signal doesn't need any processing (Esposito *et al.*, 2020). However, since the electrical activation of muscle fibers always precedes their mechanical contraction, there is an inherent electromechanical delay during muscle contraction for FMG recording. Also, in the case of the MyoWare muscle sensor, there is inbuilt hardware circuitry to provide the envelope of the signal, so no need for further processing in software. It is observed that for the 3-class pattern classification tasks, both EMG and FMG techniques give good classification accuracy. However, for 5-class and 7-class pattern classification tasks, EMG gave better results, and few classifiers provided all classification correct. For FMG, as the class increase, the same classifiers result in misclassification for lateral and medial rotation. Also, for FMG, a loose or tight setting of the FMG strap on the shank may cause a low accuracy and misclassification.

5.4 Conclusion

The authors presented a standalone computing system to classify a total of seven-foot positions by acquiring the EMG and FMG signal from four below-knee muscles. Raspberry Pi, an embedded computer that supports the ML algorithm using a Scikit-learn integrated Python module, is used to classify 3-class, 5-class, and 7-class foot movements. A 3-class pattern classification task is used to predict the foot movement in the sagittal plane, and this will be useful to control the dorsiflexion, foot-flat, and plantarflexion motion of an ankle-foot prosthesis. Out of 10 different ML algorithms, the LDA is most suitable to predict the foot positions in real-time. It is found that the EMG signal-based classification results are better as compared to FMG signal-based ankle-foot movement classification. Other than Raspberry Pi, Arduino Nano 33 BLE controller is also tested to predict the 3-class, 5-class, and 7-class foot movements. Arduino Nano 33 BLE is more advantageous due to the low prediction time (8.5msec), faster data acquisition (inbuilt analog channels), and smaller size. The embedded device-based signal acquisition, classification and control system for ankle-foot prosthesis is used to provide actuation signal for motor actuation and has a nearly real-time response. Further, the fuzzy logic algorithm is also tested for both EMG and FMG signals, and EMG provided better results in offline analysis; however, for real-time computation it resulted in poor performance when compared to TinyML. Finally, the system has been tested on a transtibial amputee, the proposed system performed well and predicted all classes in real-time, and the ankle-foot prosthesis operated properly for dorsiflexion, foot-flat, and plantarflexion foot movements.